

Electrical contact resistances of thermoelectric thin films measured by Kelvin probe microscopy

Miguel Muñoz-Rojo, Olga Caballero-Calero, and Marisol Martín-González

Citation: [Applied Physics Letters](#) **103**, 183905 (2013); doi: 10.1063/1.4826684

View online: <http://dx.doi.org/10.1063/1.4826684>

View Table of Contents: <http://scitation.aip.org/content/aip/journal/apl/103/18?ver=pdfcov>

Published by the [AIP Publishing](#)

Articles you may be interested in

[Graphene-metal contact resistivity on semi-insulating 6H-SiC\(0001\) measured with Kelvin probe force microscopy](#)

Appl. Phys. Lett. **103**, 051601 (2013); 10.1063/1.4816955

[Controlled improvement in specific contact resistivity for thermoelectric materials by ion implantation](#)

Appl. Phys. Lett. **103**, 043902 (2013); 10.1063/1.4816054

[Erratum: "Grain boundary diffusivity of Ni in Au thin films and the associated degradation in electrical contact resistance due to surface oxide film formation" \[*J. Appl. Phys.* 113, 114906 \(2013\)\]](#)

J. Appl. Phys. **113**, 169901 (2013); 10.1063/1.4803125

[Grain boundary diffusivity of Ni in Au thin films and the associated degradation in electrical contact resistance due to surface oxide film formation](#)

J. Appl. Phys. **113**, 114906 (2013); 10.1063/1.4795768

[Cathodic deposition of BiTe as thermoelectric films using choline chloride based ionic liquids](#)

AIP Conf. Proc. **1449**, 131 (2012); 10.1063/1.4731514

A promotional banner for Applied Physics Reviews. On the left is a small image of the journal cover for 'Applied Physics Reviews', showing a diagram of a layered structure. The main text 'NEW Special Topic Sections' is in large white font on a blue background. Below this, 'NOW ONLINE' is in yellow, followed by 'Lithium Niobate Properties and Applications: Reviews of Emerging Trends' in white. The AIP Applied Physics Reviews logo is in the bottom right corner.

NEW Special Topic Sections

NOW ONLINE
Lithium Niobate Properties and Applications:
Reviews of Emerging Trends

AIP Applied Physics Reviews

Electrical contact resistances of thermoelectric thin films measured by Kelvin probe microscopy

Miguel Muñoz-Rojo, Olga Caballero-Calero, and Marisol Martín-González^{a)}
*Instituto de Microelectrónica de Madrid (IMM-CNM-CSIC), c/Isaac Newton 8 (PTM),
 Tres Cantos, 28760 Madrid, Spain*

(Received 25 June 2013; accepted 8 October 2013; published online 29 October 2013)

This work presents an approach for measuring cross plane electrical contact resistances directly using Kelvin Probe Microscopy. With this technique we were able to measure the electrical contact resistances of a cross section of a thermoelectric thin film made of Bi_2Te_3 sandwiched between two gold electrodes. On the one hand, the bottom gold electrode, which is located on top of the silicon substrate, was used as a cathode in electro-deposition process to grow the sample. On the other hand, the gold electrode on top was made via physical evaporation. The electrical contact resistances measured at both interfaces were $0.11 \pm 0.01 \Omega$ and $0.15 \pm 0.01 \Omega$, respectively. These differences are related to differences between the top and bottom gold/bismuth-telluride film, obtaining smaller contact resistance where the film was grown by electro-deposition. © 2013 AIP Publishing LLC. [<http://dx.doi.org/10.1063/1.4826684>]

Thermoelectric materials have the capability to transform a difference of temperature into electricity, and vice-versa. Therefore, they can be used to take advantage of the waste heat by transforming it into electrical energy. This application makes them quite appealing for developing sustainable energy devices. The efficiency of these materials is related to their Figure of Merit (ZT), defined as $ZT = (\sigma S^2/k)T$, where σ , k , and S are the electrical conductivity, the thermal conductivity, and the Seebeck coefficient, respectively.¹ Many efforts have been made in order to improve the performance of these materials. The key to carrying out this achievement resides in the nano-structuring of materials.^{2,3} For that purpose, different experimental procedures based on electrochemistry processes, chemical and physical vapor deposition, liquid phase deposition or sputtering, etc., have allowed the fabrication of thin films and nanowires of thermoelectric materials exhibiting a high ZT .⁴

In order to evaluate the ZT of thermoelectric thin films, it is mandatory to measure and analyze the electrical and thermal conductivities of the sample, as well as their Seebeck coefficient. The measurements of the transport properties of thermoelectric nano-structured materials can be carried out separately through different experimental techniques^{5,6} or directly through the Harman method.^{7,8}

A key parameter that has to be taken into account when measuring transport properties is the influence of the electrical contacts. Indeed, when an actual thermoelectric device is implemented, the behavior of the electrical contacts may have a considerable impact on its efficiency. In fact, when passing a current through the sample the voltage drops across the contact resistances and heat is generated due to the Joule effect. Therefore, the higher the electrical resistivity of the contacts are, the more Joule heat is produced and the higher the electrical voltage drop is. This causes an alteration of the gradient of temperature in the thermoelectric sample as well as in the measurement of the Seebeck voltage. These effects are not only important for thermoelectricity, but in every

electronic device. As a matter of fact, the smaller the dimensions of the active material (thin films or nanowires), the higher the influence of the electrical contacts. Therefore, a method to accurately characterize the actual characteristics of the electrical contacts is very helpful and necessary. Although there are different methods that provide a way to determine or remove the influence of the resistance of the electrical contacts in thin films, such as the four probe technique⁹ or the variable thickness method,¹⁰ in this work we present an alternative method of measuring the electrical contact resistances directly. Additionally, works regarding measurements of contact resistance and electrical characterization with different techniques for nanowires,¹¹ molecules,¹² and polymeric or organic thin films¹³ have been reported recently.

In this work, we present a way of measuring the electrical contact resistance of a thermoelectric thin film in cross plane configuration, thanks to the Kelvin Probe Microscopy (KPM) technique.¹⁴ The cross plane direction is defined as the direction perpendicular to the surface of the substrate, that is, the direction in which the thermal gradient will be established for the device to work as a thermoelectric device in most cases. It is important to mention that the bismuth telluride films have been optimized in order to have their c -axis parallel to the surface of the substrate, that is, to have their better performance as thermoelectric material in the direction perpendicular to the surface of the substrate (cross plane direction). This technique gives the possibility of mapping the surface potential of the different components of the sample, that is, substrate, electrical contacts, and thin film, as well as a topographic image of the same region.¹⁵ The working principle of this technique consists on applying simultaneously a DC and an AC voltage through a conductive Atomic Force Microscopy tip. These voltages produce different electrostatic forces in the tip, and from the interaction of these forces with the surface under study, the local work function can be obtained.¹⁶

Previous works on KPM for in plane measurements, i.e., along the direction parallel to the surface of the substrate, of the potential drops at the contacts have been carried out for

^{a)}Electronic mail: marisol@imm.cnm.csic.es

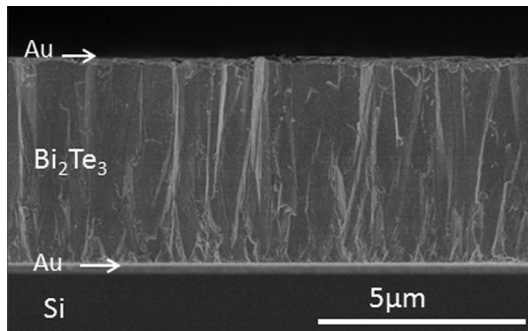


FIG. 1. Scanning electron microscope image of the edge of a $4.5\ \mu\text{m}$ thickness Bi_2Te_3 sample. Gold electrodes are placed on top and bottom of the sample.

thin film transistors.¹⁷ Nevertheless, no measurements of contact resistances in cross plane configuration have been done by this technique. In this work, we focused on the measurement of the electrical contact resistances between two gold electrodes that sandwich a Bi_2Te_3 thin film with the KPM technique.

The bismuth telluride film was grown by electrodeposition in a three electrode electrochemical cell, according to Ref. 18. The working electrode consisted of a silicon wafer (Si (110)) with an electron beam evaporated layer of 5 nm chromium and 150 nm gold layers. The reference electrode was Ag/AgCl (3M KCl), the counter electrode was a platinum mesh, and the electrochemical bath was that described in Ref. 18. The electrodeposition process was carried out at a constant applied potential of $-40\ \text{mV}$ for 2 h, resulting in a film of $4.5\ \mu\text{m}$ thickness preferentially oriented along (110). Then, a high electrical contact between the bottom gold electrode and the bismuth telluride film is granted due to the electrodeposition process itself. After electrodeposition, the sample was extracted and cleaned and then it was introduced in the same electron beam evaporation system mentioned above, and a second gold layer of 100 nm was evaporated on the surface of the film, forming the top electrode. Given that this is a physical method, the goodness of the electrical contact between this top electrode and the film depends of the conditions of the deposit, the roughness of the bismuth telluride films and other parameters,¹⁹ which make this contact different from the one obtained with the bottom electrode. Figure 1 shows a scanning electron microscope of the final sample.

Then, the Bi_2Te_3 thin film, sandwiched by two gold electrodes and held to the Si substrate, was cut and its cross

side was scanned with KPM at different bias voltages. From the obtained surface potential map, the contact resistance of the contacts was determined. For that purpose, we worked with a Cervantes Fullmode Atomic Force Microscopy (AFM) system developed by Nanotec Electrónica S.L.²⁰ and we used Multi75E-G BudgetSensors[®] probes made of Si with Cr/Pt conductive coating. This way of measuring involves many experimental requirements, e.g., the need of a considerably flat surface (in the order of nanometers), the right positioning of the tip on the electrical contacts and on the thin film and a careful adjustment of the first and second harmonic parameters of the AFM signal in order to analyze the topography and surface potential with high precision, among others. In exchange for these difficulties, one obtains the possibility to measure accurately and locally the electrical contact resistance between the electrodes and the film as well as the morphology of the sample edge.

In order to measure the cross section of the sample, a special experimental set up was developed. Conductive epoxy resist was used to connect two $50\ \mu\text{m}$ diameter gold wires on the top and bottom gold electrodes of the thin film sample. To gain access to the cross section of the sample for its measurement with the tip of the AFM, the whole sample was sandwiched between two pieces of glass of $500\ \mu\text{m}$ thickness. The pieces of glass were glued with CrystalbondTM to an alumina substrate, which was also glued to the AFM holder. Finally, the two gold wires were connected to two gold pads where other electrical wires made connection to a voltage source, which passed current through the Bi_2Te_3 film. Figure 2 shows schematically the experimental set up described above.

Moreover, it is necessary to cut along the thickness of the film in such a way that the resulting cut surface is smooth enough to carry out the KPM measurements (with a roughness on the order of nanometers), maintaining the gold of both surfaces of the film as flat as possible. Different ways of fulfilling the requirements were tried. As a first approach, the sample was broken controlling the cut with a previous scratching of the silicon substrate with a diamond tip. However, this resulted in a shearing effect.²¹ This is related to the Young and Poisson modulus of the whole sample, which is mainly dominated by the Si substrate (hardness number of around 7), given that the Bi_2Te_3 film is quite soft (hardness number of around 2.5).

A second approach consisted in an ulterior polishing of the cross section obtained after the sample was broken. For

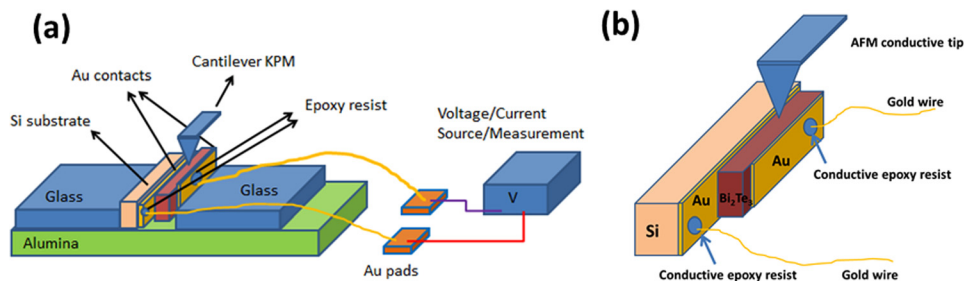


FIG. 2. (a) and (b) Schematic set up of the experimental system. The sample is sandwiched between two gold electrodes, placed on a Si substrate, and it is positioned vertically thanks to two $500\ \mu\text{m}$ pieces of laboratory glass. This system is held on an alumina substrate which is pasted on the AFM holder. A voltage source is in charge of passing a current through the sample. The KPM tip scans the sample in the current direction, i.e., in perpendicular direction to the plane of the electrodes.

that purpose, another silicon substrate of similar dimensions was glued on top of the thin film sample, in order to have the film in between two substrates of the same hardness. Then, the whole sandwich was embedded in a resist and it was polished with 0.1 μm and 0.05 μm diamond particles. However, during the polishing tension on the surface of the sample resulted in some of the thin film detaching from the bottom gold layer and the current conduction along the thin film, when using the gold layers as electrodes, was lower than expected.

Finally, we decided to improve the first method by immersing the sample into liquid nitrogen before breaking. This process resulted in a flatter cross section and required no further polishing. Even though, the Au-Bi₂Te₃ interface close to the Si substrate show in all cases a step that emerged between materials as expected from the different mechanical properties of the sample, where the AFM tip could hook on or scratch. However, it is smaller than the situation where the sample was broken without submerging it into liquid nitrogen. The average surface roughness of the Bi₂Te₃ area and its areas closer to the interfaces are around 50 nanometers, which assure accuracy when measuring.

From the theoretical point of view, the force acting at the tip in KPM measurements can be described as

$$F = \frac{1}{2} \frac{\partial C}{\partial z} U^2, \tag{1}$$

where C is the capacitance of the probe-sample system and $U = U_{dc} + U_{ac} \sin(\omega t)$ is the total potential applied. A local change in the dielectric properties would produce a change in the force signal. The resulting equation for the total force can be split in different terms

$$F = F_{dc} + F_{\omega} \sin(\omega t) + F_{2\omega} \sin(2\omega t), \tag{2}$$

where the dc term of the force is related with the topographic image of the surface of the sample, while F_{ω} and $F_{2\omega}$ are related to the surface potential and dielectric properties of the sample, respectively. The first harmonic of the ac signal, F_{ω} , can be written as

$$F_{\omega} = \frac{\partial C}{\partial z} U_{ac} U_{dc}. \tag{3}$$

Then, the dc voltage can be expressed as $U_{dc} = U_{feedback} - \phi$, where ϕ is the surface potential and the $U_{feedback}$ is the dc voltage applied by the AFM in order to

fulfill the $F_{\omega} = 0$ condition, so it can measure the sample surface potential.¹⁶

Given that the gold electrodes, the Bi₂Te₃ film and the Si substrate have different work functions, one must be able to detect differences in the surface potential given by the KPM image. Figure 3 shows a simplified profile of the expected surface potential for unbiased and biased situations.

In the unbiased situation, the KPM measures the work functions of the Bi₂Te₃ thin film and the gold electrodes. However, when a difference of voltage is applied between electrodes, the surface potential measured by the tip does not correspond only to the work function of the material scanned but also to the voltage of the scan area.

In order to measure the contact resistance between the gold electrodes and the Bi₂Te₃ thin film, it is mandatory to measure the work function difference between both materials obtained in the unbiased case, so one can subtract it in the biased situation and measure the voltage drop in the Au-Bi₂Te₃ interface.

Even though using the least aggressive way of breaking the sample, its full topographic profile has a considerable lean. Moreover, taking into account the relative large thickness of the Bi₂Te₃ thin film (4.5 μm) in comparison to the size of the electrodes (100 nm), a full KPM scan of the thin film sample should be avoided. Otherwise one would not have enough resolution to study the area of interest, which involves the interface between the electrodes and the sample giving information about the contact resistance. With this working procedure, a more accurate detection of the KPM signals is obtained, which will involve a better determination of the electrical contact resistance of the Au-Bi₂Te₃ interface.

Figure 4(a) shows a topographic image of the full cross-section of the Si/SiO₂/Au/Bi₂Te₃/Au/Air layers. Figures 4(b)–4(d) are KPM pictures of the unbiased case focused on both Au-Bi₂Te₃ interfaces and the Bi₂Te₃ film. A profile of the surface potential profile is observed from where the work function difference between materials are determined. Despite the fact that accurate difference between work function must be taken under vacuum conditions, the work function difference that we obtained experimentally under atmospheric conditions, around 140 mV and 180 mV in the Au-Bi₂Te₃ interfaces close to air and Si, respectively, is in the order of the theoretical values of the work function difference between the gold, 5.3–5.45 eV,²² and Bi₂Te₃, 5.3 eV.²³ Great care was taken in the KPM measurement of the Au-Bi₂Te₃ interface because of the step that emerged

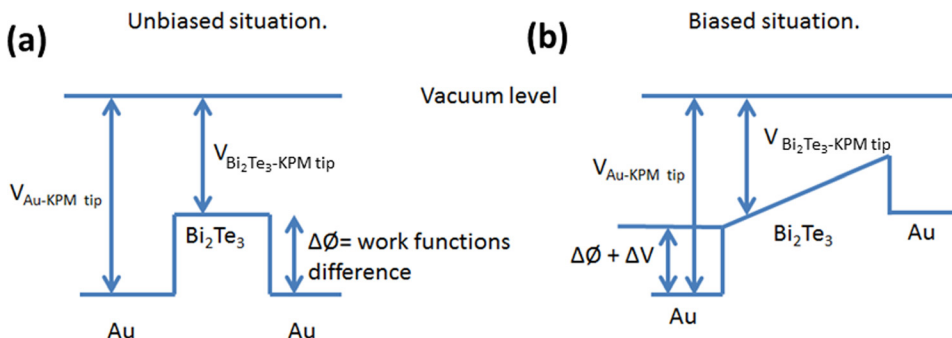


FIG. 3. Energy bands diagram of the gold electrodes and Bi₂Te₃ film at (a) unbiased and (b) biased situation.

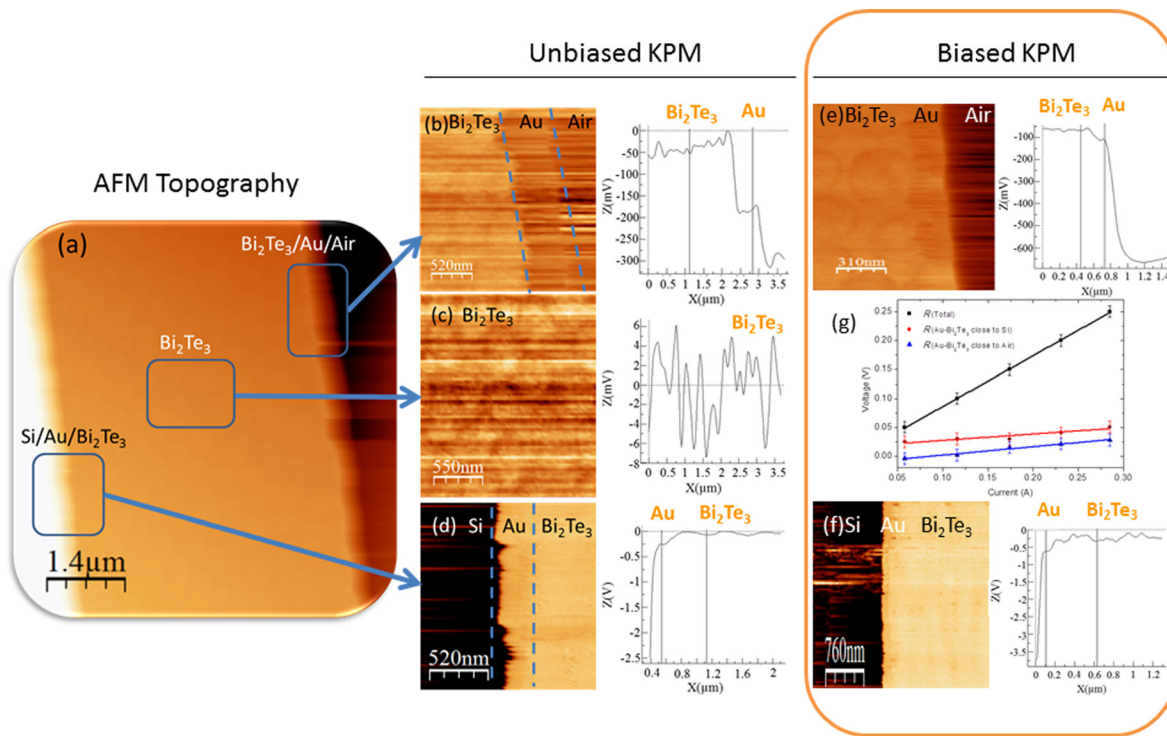


FIG. 4. (a) Topographic picture of a $4.5 \mu\text{m}$ edge of the Bi_2Te_3 thin film with gold electrodes on a Si substrate. (b) Inset picture shows a zoom of a KPM image for the unbiased edge close to air. The graph reveals the difference between the surface potential of the electrode and the Bi_2Te_3 thin film is of the order of difference between work functions $\sim 140 \text{ mV}$. (c) Inset picture shows a KPM image of the Bi_2Te_3 area. The graph shows the surface potential at this location. (d) Inset KPM picture is a zoom of the Si substrate, the gold electrode and the Bi_2Te_3 thin film. Again, the difference of surface potentials, at unbiased, is of the order of the difference between work functions as expected $\sim 180 \text{ mV}$. (e) KPM image and surface potential profile of the gold electrode and Bi_2Te_3 thin film close to air when is biased at 0.1 V . (f) KPM image and surface potential profile of the gold electrode and Bi_2Te_3 thin film close to Si substrate when is biased at 0.1 V . (g) Analysis of the electrical contact resistance after the analysis of the difference of voltage between the gold and Bi_2Te_3 thin film for different KPM images, which corresponds to biased voltages ranging from 0 V to 0.25 V . The contact resistance of the side close to the Si substrate, where the thermoelectric thin film started to grow via electro-deposition, is smaller in comparison to those closer to the air, which was deposited after the thin film was grown by gold evaporation.

between materials when breaking the sample, as it was explained above, and the similitude between their work functions.

After the work function difference is determined, multiple scans at different voltages of the same Au- Bi_2Te_3 interface were taken. The applied voltages ranged between 0.05 V and 0.3 V in steps of 0.05 V . We proceeded to measure the difference of surface potential between the gold and the Bi_2Te_3 thin film for the biased cases. Then, to obtain the voltage drop at the interface, the work function difference previously measured at zero volts was subtracted

$$\Delta V_{interface} = \Delta\phi_{\text{Au-Bi}_2\text{Te}_3}(V_{applied} \neq 0) - \Delta\phi_{\text{Au-Bi}_2\text{Te}_3}(V_{applied} = 0). \quad (4)$$

The current flowing through the sample was recorded, and applying ohms law, the contact resistance is determined

$$R_{contact} = \frac{\Delta V_{interface}}{I}. \quad (5)$$

Figures 4(e) and 4(f) show the measuring procedure and the signal obtained when a voltage of 0.1 V was applied between electrodes. A distinction between the surface potential of the gold electrode and the Bi_2Te_3 thin film is clearly observed.

The results obtained are presented in Figure 4(g). The total resistance of the system is $0.87 \pm 0.01 \Omega$, measured from the I - V curve obtained from the voltage/current

source/multimeter, which includes the intrinsic resistances of the different materials and all contact resistances present in the experimental setup, such as the epoxy contact resistances, wires resistances, etc. But the KPM is able to measure directly and locally the contact resistance at the Au- Bi_2Te_3 interfaces. At the measured voltages, the whole system and the contacts presented an ohmic behavior as shown in Figure 4(g). The electrical contact resistance of the interface closer to the air has been determined to be $0.15 \pm 0.01 \Omega$ while the one closer to the Si substrate has been found to be $0.11 \pm 0.01 \Omega$. These results show that the contact in the Au- Bi_2Te_3 interface closer to Si substrate is better than the one made by evaporation on top of the sample.

The electrical resistivity of Bi_2Te_3 thin film is around $1.5 \mu\Omega\cdot\text{m}$.²⁴ Considering a Au/ Bi_2Te_3 /Au sample area of 0.5 mm^2 and a thickness of $4.5 \mu\text{m}$, it results in an electrical resistance of around $15 \mu\Omega$. This resolution is not reached by the KPM for this kind of measurement. The resulting total electrical resistance of the whole system was determined to be $0.87 \pm 0.01 \Omega$. If subtracting the electrical resistances of the contacts, $0.15 \pm 0.01 \Omega$ and $0.11 \pm 0.01 \Omega$, we obtain a resistance for the rest of the system of $0.61 \pm 0.02 \Omega$. This resistance includes wire resistances, the resistances that arose from contacting the gold wires to the gold pads, the electrical wires used and the contact resistances from the epoxy resist, which were used to connect gold wires to the electrodes of the thin film sample. Since the resistance of Bi_2Te_3 is negligible when compared with the other resistances, we observe

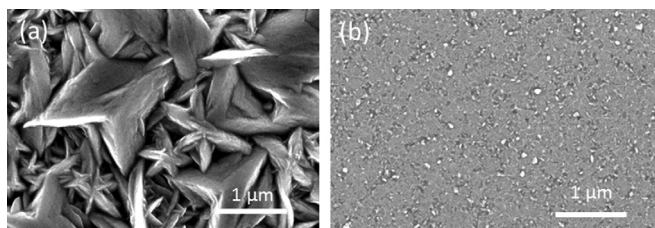


FIG. 5. SEM micrograph of a free-standing Bi_2Te_3 electrodeposited films showing the different morphologies between (a) film top part, with a r.m.s. of 70–120 nm, and (b) film bottom part of the film, with a r.m.s. of 12–22 nm.

that the total resistance measured with a two probe system is highly influenced by other electrical resistances.

Contact resistances are consequence of defects, impurities, or variation in the crystal size and orientation, formation of oxides or secondary phases at the interface between two different materials, among others. As it is mentioned in Ref. 25, the growth of a semiconductor on top of a metal, or vice-versa, does not usually involve an energy gap at its interface. However, the differences on the lattice parameters of the materials generate strains between layers, causing the dislocation of atoms and the formation of defects. Furthermore, there could be also variations in the stoichiometry of the thermoelectric compounds, as well as diffusion of the metal into the semiconductor. The transport of heat and electricity through the interface is affected considerably due to these surface features. Additionally, the formation of oxide/carboxylate/hydroxide-type phase after air exposure of the film before adding the metal contact should be contemplated in those cases where the contact is not added in high vacuum just after the film is grown.

In macroscopic devices, the values of the electrical contact resistance between a semiconductor and a metal are usually found between 10^{-8} and $10^{-9} \Omega\text{m}^2$.²⁶ This value can be compared to the ones that we have determined experimentally, $(2.8 \pm 0.1) \cdot 10^{-8} \Omega\text{m}^2$ and $(3.8 \pm 0.1) \cdot 10^{-8} \Omega\text{m}^2$ for the interface closer to Si substrate and the interface closer to air, respectively. These results are also comparable to the ohmic contacts desirable for applications in actual devices (around $10^{-9} \Omega\text{m}^2$).^{25,27–30} In order to explain this, we have to take into account that the growing method used for bismuth telluride films was electro-deposition, which involves a surface roughness¹⁸ higher than the obtained for film grown with high vacuum techniques, such as Molecular Beam Epitaxy or Metal Organic Chemical Vapor Deposition. It is also worth noting the different morphologies of the surface and the bottom of the film, as it can be clearly seen when a film is detached from the substrate, as it is shown in Figure 5. Another possible reason could be that the samples are in contact with the atmosphere before the top gold electrode was evaporated, this could lead to an oxidation of the first layers, which is avoided for sample that is grown in vacuum and straightaway gold coated without taking the sample to air. In order to determine if electrodeposited Bi_2Te_3 films samples oxidized under air exposure, they were studied over one year aging in air by different techniques like micro-RAMAN, X-ray diffraction and Rutherford back-scattering spectrometry (RBS). We have observed no oxygen containing phases within the resolution limit of each technique. So, oxidation seems not to be causing the difference.

In summary, we present a method based on KPM measurements to determine electrical contact resistances of thin films with high sensibility at the nanoscale.

With this technique we have been able to determine the contact resistances at the interfaces of a thermoelectric Bi_2Te_3 film sandwiched between gold electrodes. These values were $0.15 \pm 0.01 \Omega$ and $0.11 \pm 0.01 \Omega$, for the top and bottom electrode- Bi_2Te_3 film interfaces. The differences observed are assigned to difference of roughness between the two interfaces.

This work has been supported by ERC Starting Grant Nano-TEC number 240497 and PHOMENTA project MAT2011-27911. M.M. and O.C. acknowledge CSIC for JAE-Pre and JAE-Doc, respectively.

- ¹D. M. Rowe, *Thermoelectrics Handbook: Macro to Nano* (CRC Press, Broken Sound Parkway NW, 2005), p. 1014.
- ²J. Heremans, *Handbook of Nanotechnology* (Springer, Berlin, 2007), pp. 345.
- ³L. D. Hicks and M. S. Dresselhaus, *Phys. Rev. B* **47**(19), 12727 (1993).
- ⁴M. Martín-González, O. Caballero-Calero, and P. Diaz-Chao, *Renewable Sustainable Energy Rev.* **24**(0), 288 (2013).
- ⁵F. Völklein, V. Baier, U. Dillner, and E. Kessler, *Thin Solid Films* **187**(2), 253 (1990).
- ⁶Il-Ho Kim, *Mater. Lett.* **44**(2), 75 (2000).
- ⁷Z. X. Bian, Y. Zhang, H. Schmidt, and A. Shakouri, in *24th International Conference on Thermoelectrics* (IEEE, 2005), pp. 76–78.
- ⁸R. Singh, Z. Bian, G. Zeng, J. Zide, and J. Christofferson, *Mater. Res. Soc. Symp. Proc.* **886**, 123 (2006).
- ⁹A. Mavrokelafos, M. T. Pettes, F. Zhou, and L. Shi, *Rev. Sci. Instrum.* **78**(3), 034901 (2007).
- ¹⁰R. Venkatasubramanian, E. Siivola, T. Colpitts, and B. O'Quinn, *Nature* **413**(6856), 597 (2001).
- ¹¹M. Muñoz-Rojo, O. Caballero-Calero, A. Lopeandia, J. Rodríguez, and M. Martín-González, "Review on measurement techniques of transport properties of nanowires," *Nanoscale* (published online).
- ¹²J. M. Beebe, V. B. Engelkes, L. L. Miller, and C. D. Frisbie, *J. Am. Chem. Soc.* **124**(38), 11268 (2002).
- ¹³V. Palermo, A. Liscio, M. Palma, M. Surin, R. Lazzaroni, and P. Samori, *Chem. Commun.* **2007**(32), 3326.
- ¹⁴S. Sadewasser and T. Glatzel, *Kelvin Probe Force Microscopy* (Springer, Berlin, 2012).
- ¹⁵O. Vatel and M. Tanimoto, *J. Appl. Phys.* **77**(6), 2358 (1995).
- ¹⁶J. Colchero, A. Gil, and A. M. Baró, *Phys. Rev. B* **64**(24), 245403 (2001).
- ¹⁷K. P. Puntambekar, P. V. Pesavento, and C. D. Frisbie, *Appl. Phys. Lett.* **83**(26), 5539 (2003).
- ¹⁸M. Martín-González, A. L. Prieto, R. Gronsky, T. Sands, and A. M. Stacy, *J. Electrochem. Soc.* **149**(11), C546 (2002).
- ¹⁹C. Vicente-Manzano, A. Rojas, M. Decepeida, B. Abad, Y. Feliz, O. Caballero-Calero, D. A. Borca-Tasciuc, and M. Martín-González, *J Solid State Electrochem.* **17**(7), 2071 (2013).
- ²⁰I. Horcas, R. Fernandez, J. M. Gomez-Rodriguez, J. Colchero, J. Gomez-Herrero, and A. M. Baro, *Rev. Sci. Instrum.* **78**(1), 013705 (2007).
- ²¹A. K. Kaw, *Mechanics of Composite Materials* (CRC Press, Boca Raton, FL, United States, 2006).
- ²²W. M. H. Sachtler, G. J. H. Dorgelo, and A. A. Holscher, *Surf. Sci.* **5**(2), 221 (1966).
- ²³D. Haneman, *J. Phys. Chem. Solids* **11**(3–4), 205 (1959).
- ²⁴F. Xiao, C. Hangarter, B. Yoo, Y. Rheem, K.-H. Lee, and N. Myung, *Electrochim. Acta* **53**(28), 8103 (2008).
- ²⁵L. W. da Silva and M. Kaviany, *Int. J. Heat Mass Transfer* **47**(10–11), 2417 (2004).
- ²⁶F. Li, X. Huang, W. Jiang, and L. Chen, *AIP Conf. Proc.* **1449**(1), 458 (2012).
- ²⁷S.-P. Feng, Y.-H. Feng, J. Chang, B. Yang, B. Poudel, Z. Yu, G. Ren, and G. Chen, *Phys. Chem. Chem. Phys.* **15** (18), 6757 (2013).
- ²⁸A. M. Pettes, R. Melamud, S. Higuichi, and K. E. Goodson, in *26th International Conference on Thermoelectrics* (IEEE, 2007).
- ²⁹D. E. Wesolowski, R. S. Goeke, A. M. Morales, S. H. Goods, P. A. Sharma, M. P. Saavedra, K. R. Reyes Gil, and C. A. Appleby, *J. Mater. Res.* **27**(8), 1149 (2012).
- ³⁰E. Preisler, J. Bayersdorfer, M. Brunner, J. Bock, and S. Elschner, *Supercond. Sci. Technol.* **7**(6), 389 (1994).